COMPLEMENTARY METHODS FOR CHARACTERISING SLICK ROCK AEOLIAN SANDSTONE

S. Baraka-Lokmane, I. Main, S. Elphick, B. Ngwenya
Department of Geology & Geophysics, University of Edinburgh, UK

INTRODUCTION

The petrophysical properties of sandstones, such as wettability, porosity, degree of saturation, and absolute and/or relative permeabilities, are all affected by the microstructural properties of the rock. These include: the nature of the constituent minerals and cement, the degree of rock cementation; the degree of sorting or equivalently the particle size distribution of the grains; and the pore-size distribution. We characterise and analyse the rock samples both before and after a series of two-phase (brine/oil) flow experiments reported elsewhere in this volume (Jones et al., 2001), and analyse the chemical constituents of the exit brine. This procedure is designed to establish the underlying cause for any correlation between the changes in microstructure and any observed changes both in absolute permeability and/or relative permeabilities of the oil/water phases. Sixteen samples of Slick Rock Aeolian sandstone were chosen for this study. The methods used include Magnetic Resonance Imaging (MRI), Nuclear Magnetic Resonance (NMR), X-ray Computer Tomography (CT) Scanning, particle size analysis, point counting based on petrographic thin sections, Environmental Scanning Microscopy (ESEM), X-Ray Diffraction (XRD), and X-Ray Fluorescence (XRF). The results of the different methods used were found to be consistent with each other, but the combination of a variety of methods has allowed a full characterisation of the rock and the pore fluid.

NUCLEAR MAGNETIC RESONANCE (NMR) AND MAGNETIC RESONANCE IMAGING (MRI) MEASUREMENTS

NMR has long been used in the oil industry for the measurement of petrophysical rock properties. These include the bulk porosity (Cowgill et al., 1981) and the distribution of pore size (Kenyon, 1989) and fluid saturation (Baldwin and Yamanashi, 1991). In this study we have carried out MRI and NMR measurements before and after flow tests to determine changes in water saturations, porosity and pore size distribution. Unfortunately, no images could be obtained using conventional MRI at 4.7 T, because the transverse relaxation time T2* was reduced dramatically by the presence of iron in the sample. Instead, we used the continuous-wave magnetic resonance imaging (CW-MRI) technique (Lurie et al., 1996) to visualise water imbibition by capillary action in the sample. The results clearly show the development of water front (Figure 1). Initially the water front is concave (first image). This water front spreads out slowly on subsequent images. (Second-order local fluctuations in the amplitude of the signal are due to amplification of background noise during digital data processing). We attempted to determine the porosity and the pore size distribution in the samples using a GE Ω CSI spectrometer operating for proton resonance at 85 MHz at 100 % saturation in brine, using transverse relaxation

back to contents

NMR. The measured parameters are not physically realistic, due to the contamination of the core by a significant amount of iron. We conclude that NMR and MRI measurements are not suitable for this rock type, most likely due to a combination of the total iron content and its large spatial heterogeneity within the samples. Experiments are currently under way with sandstone core of a low iron content to see if the method can be used to characterise a flood front in this case.

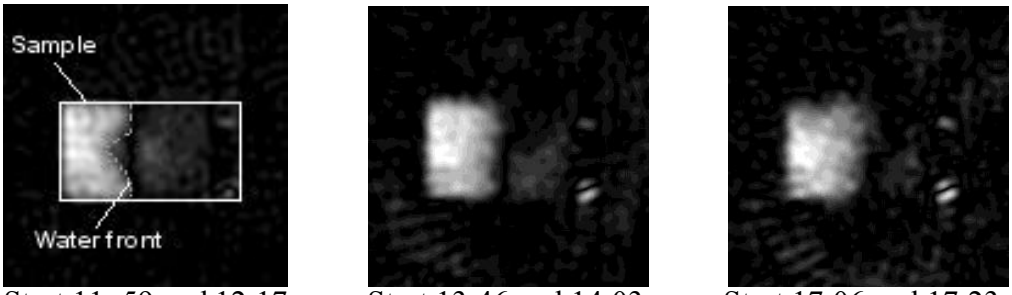

Start 11: 59 end 12:17 Start 13:46 end 14:03 Start 17:06 end 17:23

Figure 1. Development of the water front inside sample 8 of the Slick Rock Aeolian sandstone.

X-RAY COMPUTER TOMOGRAPHY (CT-SCANNING)

This scanning technique is useful in the observation of both heterogeneous and apparently homogeneous lithologies. The following features can be characterised: bedding features and sedimentary structures, natural and coring-induced fractures, cement distribution, small scale grain size variation, and density variation. On the different images shown in Figures 2 and 3, the different mineral phases are recognisable: calcite in white, microcline in light grey, quartz in dark grey and iron in near-white. On Figure 2, the distribution of calcite cement is very heterogeneous, being distributed in white patches or layers, and iron banding is seen in the near-white layers. Figure 3 clearly shows a horizontal calcite-filled fracture in the upper half of sample 13. This diageneticaly-sealed fracture is perpendicular to the bore core axis, and could constitute a barrier to vertical flow. This inference will be checked directly after the flow using more destructive methods (i.e. resin impregnation and sectioning). We conclude that the method is particularly useful for imaging calcite and hematite. The finite presence of heterogeneously-distributed hematite implied by the null MRI results is confirmed.

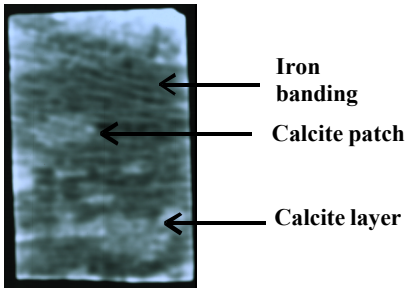

Figure 2. Slice 2 of sample 4 showing the location of iron banding and calcite cement.

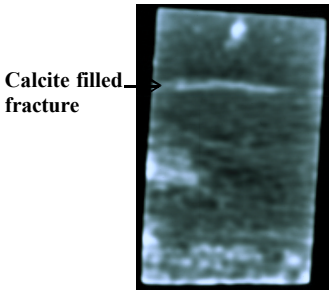

Figure 3. Slice 3 of sample 13 showing a fracture filled with calcite.

ENVIRONMENTAL SCANNING ELECTRON MICROSCOPY (ESEM) MEASUREMENTS

The ESEM technique was used to determine the wettability of the different minerals before and after the two-phase flow tests. An indication of wettability can be obtained through examination of the contact angle formed between a solid surface and a droplet of fluid on that surface, with the angle being recorded through the denser fluid (Gauchet et al., 1993; Robin and Cuiec, 1998; Buckman et al., 2000). In our study interstitial illite particles, or quartz and feldspar minerals covered by illite, are all very water wet. Fresh surfaces of quartz and feldspar are water wet (low contact angles, lower than 90^o) (Figure 4), and uncemented quartz is intermediate water wet (contact angle $\approx 90^o$) (Figure 5).

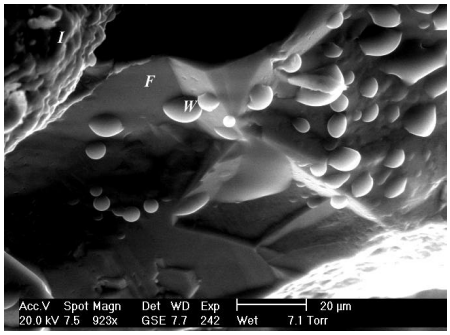

Figure 4. ESEM photo of a feldspar Crystal, showing the low dome shaped droplets of water on the feldspar.

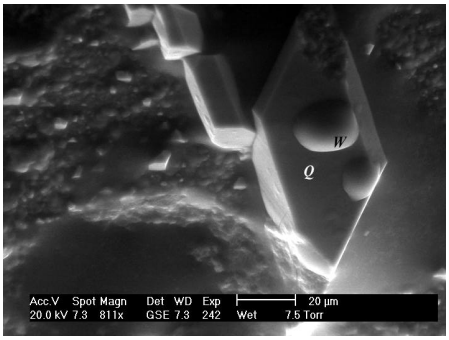

Figure 5. ESEM photo of quartz rhombs, showing the dome shape of water droplets with intermediate contact angles.

PETROGRAPHY AND POROSITY ESTIMATION

The Slick rock Aeolian sandstone samples present a clear tint in hand specimen. The grains are rounded, well sorted and friable. Thin sections of the rock sample were point-counted according to mineral phase and pore space using a grid of 400 sample points. The mineral results plot in the quartz arenite and sub arkose range of the Quartz-Feldspar-Rock Fragment field. Cements are in the form of clay minerals (mainly illite), hematite interspersed with illite, carbonate (calcite), and quartz and feldspar in the form of overgrowths. Hematite cementation, when it is present, is interspersed with clays around the detrital grains. Its presence at less than 1 % is still large enough to spoil the NMR measurements. The 2-D porosity from the point-counting varies between 20 % and 23 % and is more homogeneously distributed than the cement, which varies between 5 % to 18 % of the sample volume. Modern imaging software was also used in order to obtain quantitative 2-D porosity values of digitised thin-section images using a desktop computer. Ten images were taken for each sample and an arithmetic mean calculated from the individual estimates. The results are similar to those calculated using the point-counting method, but are more accurate (19.34 % and 23.54 %).

PARTICLE SIZE ANALYSIS, X-RAY DIFFRACTION (XRD) AND X-RAY FLUORESCENCE (XRF) ANALYSES

The particle size distribution curves of the Slick Rock Aeolian sandstone samples show that the samples are well graded between clay, silt and fine sand fractions. The coefficient of sorting S_o is less than 1.4. The particle size distribution is heterogeneous, with a coefficient of uniformity U_c greater than 2. The mean grain size varies between 204.2 mm and 216.8 mm. XRD analyses were carried out both on whole rock and the fine particle fraction in order to quantify the mineralogy independently from the point counting exercise. The results are consistent with the point-counting exercise. XRF analyses of the samples were also used to determine the chemical composition of the samples using off-cuts before the flow tests, confirming the presence of iron oxide. This means that some diagenetic dissolution of Fe_2O_3 might in principle occur during the flow tests. In practice, no significant diagenetic dissolution of Fe_2O_3 was seen in the exit pore fluid during the flow tests.

CONCLUSIONS

Several complementary and overlapping methods have been used in this study to characterise Slick Rock Aeolian sandstones. This strategy allows a full range of characteristics to be determined, with internal checking between measurements. The results of the different methods used were found to be consistent with each other. The finite and heterogeneous nature of iron in the sample is confirmed independently by the CT scans and by the absence of a resolvable signal in the NMR and MRI measurements. Likewise, the determination of the mineralogical composition of the samples, the type and the abundance of the cements, and particularly the location and the abundance of the calcite and hematite, are all well characterised by several independent methods. Future work will analyse the rock samples after two-phase (brine/oil) flow tests, in order to demonstrate the influence of the measured characteristics on the observed fluid-rock interactions under stress. In particular the methods will be used to determine the correlation between changes in microstructure and the observed changes in absolute and/or relative permeabilities of the oil/water phases.

ACKNOWLEDGEMENTS

This work was funded by Engineering and Physical Sciences Research Council, grant: GR/M6 2150, with support from Exxon-Mobil, BP Amoco, DTS and RML.

REFERENCES

Baldwin, B.A. and Yamanashi, W.S. (Sept.-Oct. 1991): NMR Imaging of Fluid Saturation Distributions in Cores – The Log Analyst, Pp 536-549.

Buckman, J.O., Todd, A.C. and Hill, P.I. (2000): Observations on Reservoir Rock Wettability Using an Environmental Scanning Electron Microscope – Microscopy and Analysis, Pp 35-37.

Cowgill, D.F., Pitman, J.K. and Seevers, D.O. (May 1981): NMR Determination of Porosity and Permeability of Western Tight Gas Sands – SPE/DOE 9875, presented at Low Permeability Symposium, Denver, Colorado.

Gauchet, R., Chenevière, P. and Tricart, J-P. (1993): Visualisation of rock samples in their state using environmental scanning electron microscope – SCA Conference, Paper Number 9304, Pp 1-14.

Kenyon, W.E., Howard, J.J., Sezginer, A., Straley, C., Matteson, A., Horkowitz, K. and Ehrlich, R. (1989): Pore-size Distribution and NMR in Microporous Cherty Sandstones – SPWLA Annual logging symposium.

Lurie, D.J., McCallum, S.J., Hutchison, J.M.S. and Alecci, M. (1996): Continuous-wave NMR imaging of solids – Magma, n^{o} 4, Pp 77-81.

Robin, M. and Cuiec, L. (Nov 1998): Two SEM Techniques to Investigate Reservoir-Rock Wettability – JPT, Pp 77-79.

back to contents